J|A|C|S
ARTICLES
Published on Web 05/08/2007

Counting the Monomers in Nanometer-Sized Oligomers by Pulsed Electron−Electron Double Resonance

Bela E. Bode,[†] Dominik Margraf,[†] Jörn Plackmeyer,[†] Gerd Dürner,[‡] Thomas F. Prisner,[†] and Olav Schiemann*,[†]

Contribution from the Institute of Physical and Theoretical Chemistry, Center for Biomolecular Magnetic Resonance, and Institute of Organic Chemistry and Chemical Biology, Max-von-Laue-Strasse 7, J. W. Goethe-University, 60438 Frankfurt am Main, Germany

Received August 9, 2006; E-mail: olav.schiemann@prisner.de

Abstract: In a lot of cases active biomolecules are complexes of higher order, thus methods capable of counting the number of building blocks and elucidating their geometric arrangement are needed. Therefore, we experimentally validate here spin-counting via 4-pulse electron−electron double resonance (PELDOR) on well-defined test samples. Two biradicals, a symmetric and an asymmetric triradical, and a tetraradical were synthesized in a convergent reaction scheme via palladium-catalyzed cross-coupling reactions. PELDOR was then used to obtain geometric information and the number of spin centers per molecule in a single experiment. The measurement yielded the expected distances (2.2−3.8 nm) and showed that different spin−spin distances in one molecule can be resolved even if the difference amounts to only 5 Å. The number of spins *n* has been determined to be 2.1 in both biradicals, to 3.1 and 3.0 in the symmetric and asymmetric triradicals, respectively, and to 3.9 in the tetraradical. The overall error of PELDOR spin-counting was found to be 5% for up to four spins. Thus, this method is a valuable tool to determine the number of constituting spin-bearing monomers in biologically relevant homo- and heterooligomers and how their oligomerization state and geometric arrangement changes during function.

Introduction

There is a growing interest in the study of large protein−protein complexes in membranes. For example, it is known from crystal structures that ion-channels and transporters,[1] like the the ClC chloride channel, potassium channels, or glutamate transporters, are complexes comprising two or more monomeric protein units.[2] For other ion-channels or transporters, like the polypeptide antibiotic Antiamobin,[3] the number of constituting monomers have been proposed on the basis of molecular modeling but not verified experimentally. Furthermore, several signal-transduction proteins like the fumarate sensor DcuS[4] are only active in membranes, where it is proposed to form a specific homo-oligomer. The number of constituting monomers is, however, unknown. Another highly debated topic is the question whether membrane-bound electron-transfer proteins of the respiratory chain form super complexes[5] to enable fast and reliable interprotein electron transport. Also, a huge machinery that depends on the binding of several proteins during the catalytic cycle is the RNA processing spliceosome.[6] The number and type of interacting partners change from state to state through the process of RNA cleavage and ligation. For several of these functional states it is not fully understood how many and which proteins are involved.

One method that can be employed to investigate the number of monomers in a oligomer is X-ray crystallography. However, it is still demanding to obtain suitable single crystals of large complexes, and it has not yet been possible to crystallize them within membranes. Therefore, complementary biophysical methods capable of measuring the number of interacting monomers in the presence or absence of a membrane, like cryo-electron microscopy,[7] are needed. In solution, electrospray ionization mass spectrometry is a well-established method for the determination of such noncovalent interactions.[8] Two other methods also enabling extraction of the number of constituting units in solution are confocal time correlated fluorescence spectroscopy[9] and, as shown recently, fluorescence resonance energy transfer (FRET).[10] In addition, dynamic light scattering can be employed to monitor soluble aggregates and oligomers

[†] Institute of Physical and Theoretical Chemistry, Center for Biomolecular Magnetic Resonance.
[‡] Institute of Organic Chemistry and Chemical Biology.

(1) (a) MacKinnon, R. *Angew. Chem., Int. Ed.* **2004**, *43*, 4265. (b) Gouaux, E.; MacKinnon, R. *Science* **2005**, *310*, 1461.
(2) (a) Langosch, D.; Thomas, L.; Betz, H. *Proc. Natl. Acad. Sci. U.S.A.* **1988**, *85*, 7394. (b) Páli, T.; Finbow, M. E.; Holzenburg, A.; Findlay, J. B. C.; Marsh, D. *Biochemistry* **1995**, *34*, 9211. (c) Iwamoto, H.; Czajkowsky, D. M.; Cover, T. L.; Szabo, G.; Shao, Z. *FEBS Lett.* **1999**, *450*, 101. (d) Czajkowsky, D. M.; Iwamoto, H.; Coverdagger, T. L.; Shao, Z. *Proc. Natl. Acad. Sci. U.S.A.* **1999**, *96*, 2001.
(3) O'Reilly, A. O.; Wallace, B. A. *J. Peptide Sci.* **2003**, *9*, 769.
(4) Janausch, I. G.; Garcia-Moreno, I.; Unden, G. *J. Biol. Chem.* **2002**, *277*, 39809.
(5) (a) Schägger, H. *Biochim. Biophys. Acta* **2002**, *1555*, 154. (b) Stroh, A.; Anderka, O.; Pfeiffer, K.; Yagi, T.; Finel, M.; Ludwig, B.; Schägger, H. *J. Biol. Chem.* **2004**, *279*, 5000.
(6) Will, C. L.; Lührmann, R. In *RNA World*, 3rd ed.; Gesteland, R. F., Cech, T. R., Atkins, J. F., Eds.; Cold Spring Harbor: New York, 2006; pp 369.
(7) Dube, P.; Herzog, F.; Gieffers, C.; Sander, B.; Riedel, D.; Müller, S. A.; Engel, A.; Peters, J.-M.; Stark, H. *Mol. Cell* **2005**, *20*, 867.
(8) (a) Rostom, A. A.; Robinson, C. V. *Curr. Opin. Struct. Biol.* **1999**, *9*, 135. (b) Daniel, J. M.; Friess, S. D.; Rajagopalan, S.; Wendt, S.; Zenobi, R. *Int. J. Mass Spectrom.* **2002**, *216*, 1.

10.1021/ja065787t CCC: $37.00

by their hydrodynamic properties.[11] First approaches in liquid-[12] and solid-state[13] nuclear magnetic resonance (NMR) are published. In this study, we show experimentally that also pulsed electron−electron double resonance (PELDOR)[14] can be used to count the number of interacting monomers in a complex.

PELDOR is a reliable method to measure interspin distances in the nanometer range[15] between nitroxide spin labels[16] or native spin centers in biomolecules.[17] Milov, Tsvetkov, et al. proposed in 1984 that PELDOR can not only be used to measure spin−spin distances but, in addition, to count the number of coupled spins from the modulation depth[18] and used this to postulate the aggregation state of small peptides.[19] However, up to now there is no report on the experimental verification of spin-counting by PELDOR using fully characterized test systems. Therefore, we describe herein the synthesis of suitable model systems mimicking different geometries and aggregation states of biomolecules and use the model systems to evaluate the method with respect to accuracy and limitations for biological applications.

Methods and Materials

Synthesis. Coupling reactions and deprotection steps were carried out applying standard Schlenk techniques under argon atmosphere. All explicit synthesis procedures are given in the Supporting Information. Dry toluene was degassed by several freeze−thaw cycles. Benzene was distilled from sodium metal, and amines were distilled from CaH_2 both under argon atmosphere. Dry DMF was degassed with argon.

Analytic relied on elemental analysis and mass spectrometry such as EI, ESI, and MALDI. EI mass spectra were recorded on a CH7A spectrometer from MAT. ESI mass spectra were acquired on a LCQ Classic spectrometer from Thermo Electron and MALDI mass spectra on a Voyager DE-Pro or STR spectrometer from Applied Biosystems. Proton nuclear magnetic resonance spectra of diamagnetic molecules were acquired at 250 MHz on a Bruker AM-250 spectrometer and calibrated using residual nondeuterated solvents as internal standard (δ $CHCl_3$ = 7.240). IR spectra were recorded on a Jasco FTIR 420 spectrometer using KBr pellets. Analytical HPLC was carried out with a Waters 590 pump, a Waters UV detector 440, and Waters refractometer detector 410 on Macherey-Nagel Nucleosil 50−10 columns. Elemental analysis was performed on a Foss-Heraeus CHN-O-Rapid.

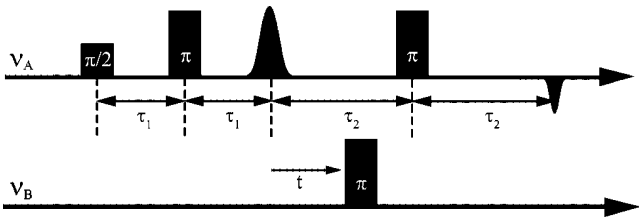

Figure 1. Pulse sequences for 4-pulse ELDOR.

PELDOR Methodology. All following spin-counting experiments were done with the 4-pulse ELDOR pulse sequence shown in Figure 1.

The pulses at the detection frequency ν_A create an echo from the spins on resonance, named in the following as A spins. Introduction of an inversion pulse at the pump frequency ν_B flips spins resonant with this second frequency, here defined as B spins. Thus, a coupling ω_{AB} between A and B spins causes a shift in the Lamor frequency of the A spins by ω_{AB} and therefore a change in the echo signal $V(t)$. The resulting PELDOR signal ($V(t)$) can be considered as a product of two contributions:

$$V(t) = V_{intra}V_{inter} \tag{1}$$

V_{intra} describes all spins coupled in one spin cluster, whereas V_{inter} takes into account the signal decay caused by a homogeneous distribution of the clusters in the sample. Assuming that the spin-orientations are not changed because of spin diffusion or spin−lattice relaxation, V_{intra} can be described by eq 2.[18]

$$V(t)_{intra} = \frac{1}{n}\left\langle \sum_{A=1}^{n} \prod_{\substack{B=1 \\ B\neq A}}^{n} (1 - \lambda_B(1 - \cos(\omega_{AB}t))) \right\rangle \tag{2}$$

with

$$\omega_{AB} = \omega_{dd} + 2\pi J_{AB} \tag{3}$$

and

$$\omega_{dd} = -\frac{\mu_0 \hbar}{4\pi} \frac{\gamma_A \gamma_B}{r_{AB}^3}(3\cos^2\theta - 1) \tag{4}$$

where n is the number of radicals per cluster, λ_B is the fraction of B spins inverted by the pump pulse, t is the time delay of the pump pulse, ω_{dd} is the full dipole−dipole splitting, μ_0 is the vacuum permeability, γ are the magnetogyric ratios of the spins, $\hbar$ is the Planck constant divided by 2π, r_{AB} is the distance between the spins, θ is the angle between r_{AB} and the external magnetic field, J_{AB} is the exchange coupling in units of Hz, and $\langle ... \rangle$ is the averaging over values of r_{AB}, J_{AB}, and θ. We assume J_{AB} to be negligible versus ω_{dd} and also that the radical centers in a cluster do not bear any angular correlation.

Considering a random distribution of clusters and neglecting excluded volumes, V_{inter} can be written as eq 5.[20]

$$V(t)_{inter} = \exp\left(-\frac{2\pi\gamma_A\gamma_B\mu_0}{9\sqrt{3}\hbar} c\lambda_B t\right) \tag{5}$$

Here c is the radical concentration in m^{-3}.

Thus, the coupling between spins can be deduced parameter-free from the time domain signal by division of $V(t)$ by V_{inter} and cosine Fourier transformation. In disordered samples a broad distribution of

(9) (a) Heinze, K. G.; Jahnz, M.; Schwille, P. *Biophys. J.* **2004**, *86*, 506. (b) Becker, C. F. W.; Seidel, R.; Jahnz, M.; Bacia, K.; Niederhausen, T.; Alexandrov, K.; Schwille, P.; Goody, R. S.; Engelhard, M. *Chem. Bio. Chem.* **2006**, *7*, 891.
(10) (a) Liu, J.; Lu, Y. *J. Am. Chem. Soc.* **2002**, *124*, 15208. (b) Watrob, H. M.; Pan, C.-P.; Barkley, M. D. *J. Am. Chem. Soc.* **2003**, *125*, 7336.
(11) (a) Nag, N.; Krishnamoorthy, G.; Rao, B. J. *FEBS J.* **2005**, *272*, 6228. (b) Chugh, J.; Chatterjee, A.; Kumar, A.; Mishra, R. K.; Mittal, R.; Hosur, R. V. *FEBS J.* **2006**, *273*, 388. (c) Cramer, J.; Jaeger, J.; Restle, T. *Biochemistry* **2006**, *45*, 3610.
(12) Krishnan, V. V. *J. Magn. Reson.* **1997**, *124*, 468.
(13) Luo, W.; Hong, M. *J. Am. Chem. Soc.* **2006**, *128*, 7242.
(14) Milov, A. D.; Salikov, K. M.; Shirov, M. D. *Fiz. Tverd. Tela* **1981**, *23*, 975.
(15) (a) Larsen, R. G.; Singel, D. J. *J. Chem. Phys.* **1993**, *98*, 5134. (b) Martin, R. E.; Pannier, M.; Diederich, F.; Gramlich, V.; Hubrich, M.; Spiess, H. W. *Angew. Chem., Int. Ed.* **1998**, *37*, 2833.
(16) (a) Jeschke, G. *Macromol. Rapid Commun.* **2002**, *23*, 227. (b) Schiemann, O.; Weber, A.; Edwards, T. E.; Prisner, T. F.; Sigurdsson, S. T. *J. Am. Chem. Soc.* **2003**, *125*, 3434. (c) Schiemann, O.; Piton, N.; Mu, Y.; Stock, G.; Engels, J. W.; Prisner, T. F. *J. Am. Chem. Soc.* **2004**, *126*, 5722. (d) Zhou, Z.; DeSensi, S. C.; Stein, R. A.; Brandon, S.; Dixit, M.; McArdle, E. J.; Warren, E. M.; Kroh, H. K.; Song, L.; Cobb, C. E.; Hustedt, E. J.; Beth, A. E. *Biochemistry* **2005**, *44*, 15115.
(17) (a) Bennati, M.; Robblee, J. H.; Mugnaini, V.; Stubbe, J.; Freed, J. H.; Borbat, P. *J. Am. Chem. Soc.* **2005**, *127*, 15014. (b) Kay, C. W. M.; Elsässer, C.; Bittl, R.; Farell, S. R.; Thorpe, C. *J. Am. Chem. Soc.* **2006**, *128*, 76. (c) Elsässer, C.; Brecht, M.; Bittl, R. *J. Am. Chem. Soc.* **2002**, *124*, 12606. (d) Hara, H.; Kawamori, A.; Astashkin, A. V.; Ono, T.-A. *Biochim. Biophys. Acta* **1996**, *1276*, 140.
(18) (a) Milov, A. D.; Ponomarev, A. B.; Tsvetkov, Y. D. *Chem. Phys. Lett.* **1984**, *110*, 67. (b) Milov, A. D.; Maryasov, A. G.; Tsvetkov, Y. D. *Appl. Magn. Reson.* **1998**, *15*, 107.
(19) Milov, A. D.; Tsvetkov, Y. D.; Formaggio, F.; Crisma, M.; Toniolo, C.; Raap, J. *J. Am. Chem. Soc.* **2000**, *122*, 3843.
(20) Mims, W. B. In *Electron Paramagnetic Resonance*; Geschwind, S., Ed.; Plenum: New York, 1972; pp 263.

ω_{AB} values exists. Therefore, the $\langle\cos(\omega_{AB}t)\rangle$ terms in eq 2 will interfere to zero for times $t \gg \omega_{AB}^{-1}$, and V_{intra} will tend to its limit V_λ, which is the value of V_{intra} when all modulation is damped. Assuming that all B spins are of similar nature, V_λ can be written in the form of

$$V_\lambda = (1 - \lambda_B)^{(n-1)} \quad (6)$$

Thus, V_λ values factorize under the conditions given above, for example, a triradical can be described as the square of a biradical and a tetraradical as the cube of a biradical. This approximation will not be valid if the coupling spins belong to radicals with different spectral widths. In that case the different λ_B values have to be taken into account explicitly.

From eq 6 follows that the number of radicals in a cluster is

$$n = \frac{\ln V_\lambda}{\ln(1 - \lambda_B)} + 1 \quad (7)$$

If $\lambda \ll 1$, then eq 6 can be approximated linearly to eq 8:[18a]

$$V_\lambda = 1 - \lambda_B(n - 1) \quad (8)$$

The only free parameter in the calculation of n is λ_B, which can be determined experimentally using a standard biradical. In case of strong angular correlations different λ_B values for each A−B pair in eq 2 have to be explicitly taken into account. The extent of such effects will be discussed in the results section.

Pulse EPR Measurements. All samples were prepared from solutions of radicals **1**−**6** in d_8-toluene (100 μM in spins, 80 μL). The samples were saturated with argon prior to rapid freezing and storage in liquid nitrogen. Mixtures of radicals were obtained by combining d_8-toluene solutions of the pure substances after determination of their concentrations by cw-EPR. All PELDOR spectra were recorded on a Bruker ELEXSYS E580 pulsed X-band EPR spectrometer with a standard flex-line probe head housing a dielectric ring resonator (MD5 W1) equipped with a continuous flow helium cryostat (CF935) and temperature control system (ITC 502) both from Oxford instruments. The second microwave frequency was coupled into the microwave bridge by a commercially available setup (E580-400U) from Bruker. All pulses were amplified via a pulsed travelling wave tube (TWT) amplifier (117X) from Applied Systems Engineering. The resonator was over-coupled to a quality factor Q of about 50. Four-pulse ELDOR experiments were performed with the pulse sequence $\pi/2(\nu_A)$-τ_1-π-(ν_A)-$(\tau_1 + t)$-$\pi(\nu_B)$-$(\tau_2 - t)$-$\pi(\nu_A)$-τ_2-echo. The pump pulse (ν_B) was set to 12 ns at the resonance frequency of the resonator and applied to the maximum of the nitroxide spectrum, where it selects the central $m_I = 0$ transition of A_{zz} together with the $m_I = 0, \pm1$ transitions of A_{xx} and A_{yy}. The pulse amplitude was optimized on maximum inversion of a Hahn-echo on the pump frequency. Detection pulses (ν_A) were set to 32 ns and applied at 70 MHz higher frequency. The amplitude was chosen to optimize the refocused echo. The $\pi/2$-pulse was phase-cycled to eliminate receiver offsets. All spectra were recorded at 40 K with an experiment repetition time of 5 ms, a video amplifier bandwidth of 25 MHz and an amplifier gain of 60 dB. For quantitative measurements of the modulation depth τ_1 was set to 400 ns and τ_2 to 5200 ns. Usually 1000 scans were accumulated with 272 data points and time increments Δt of 20 ns giving an approximate measurement time of 1 h. All spectra were acquired using the same experimental parameters as quality factor of the resonator, pulse amplitudes, and timings. Spectra for low λ_B were measured using the same conditions but with an inversion pulse of 92 ns and a τ_2 of 4400 ns. Suppression of proton modulation by the addition of 8 spectra of variable τ_1 with Δt_1 of 8 ns was done for comparative reasons. (These data are only shown in the Supporting Information.) Transverse relaxation times and the corresponding scaling factors for **1**−**6** were estimated by comparing the Hahn echo and refocused echo amplitudes (40960 averages each) using the same 3-pulse sequence as for the detection sequence in the PELDOR measurements (for details see Supporting Information). Tikhonov regularizations were performed on spectra with τ_2 of 6−8 μs with time increments Δt of 8−12 ns to increase the resolution of the distance transformations. All spectra for quantification of the modulation depth were divided by a monoexponential decay and normalized to the point $t = 0$. These preprocessed datasets were also taken for cosine Fourier transformation. λ_B was calibrated using standard biradicals; it was determined to be 0.43 and 0.12 for a 12 and a 92 ns inversion pulse, respectively.

Simulation of PELDOR Time Domain Data. Simulations were performed based on eq 2−5, with detection and pumping efficiencies explicitly calculated for each orientation and nitrogen hyperfine state. The respective resonance positions are computed based on the g and hyperfine tensor of the monomeric nitroxide spin label from literature[21] and the experimental values for pulse lengths and microwave frequency. Full rotational freedom about the acetylene linkers and backbone bending of ±10° weighted with a $\cos^2$ profile was assumed and 10 000 structures generated. Excitation profiles were calculated with the analytic expression for rectangular pulses. Powder averages are performed with 12 300 equally distributed points on the half sphere.

Results and Discussion

Synthesis of Model Systems. Suitable model systems for PELDOR spin-counting should be chemically stable and rigid and have a spin−spin distance that is well within the limit of the method (15−80 Å).[16a,22] The polynitroxide radicals **1**−**5** (Scheme 1) containing fairly rigid ethynyl substituted aromatic spacers fulfill these requirements. In addition, the use of these spacers allowed us to synthesize molecules **1**−**5** from a small pool of building blocks.

The nitroxide 3-ethynyl-1-oxyl-2,2,5,5-tetramethylpyrroline **6**, which is commonly used as a spin label for RNA or DNA,[16c,23] was employed as the spin-bearing group. It was prepared from 2,2,6,6-tetramethyl-4-oxopiperidine[24] in slight modification to to the procedure described by Hideg et al.[25] Molecule **6** was converted to the polyradical precursor **9** via the coupling and protection sequence shown in Scheme 2. We decided to first attach a protected acetylene to 4,4′-diiodobiphenyl and add the nitroxide spin-label **6** in a second step for reasons of synthesis economy, as **6** has to be synthesized in eight steps. Because the nitroxyl moiety is easily reduced or oxidized,[26] a protective group strategy for acetylene units and cleavage conditions not interfering with the nitroxyl functionality had to be applied. Here, we chose the polar protecting group 2-hydroxypropyl, because it facilitates separation via column chromatography in contrast to unpolar protecting groups as trimethylsilane.[27] We favored the 2-hydroxypropyl group over

(21) Fritscher, J.; Beyer, M.; Schiemann, O. *Chem. Phys. Lett.* **2002**, *364*, 393.
(22) Jeschke, G. *Chem. Phys. Chem.* **2002**, *3*, 927.
(23) (a) Spaltenstein, A.; Robinson, B. H.; Hopkins, P. B. *J. Am. Chem. Soc.* **1988**, *110*, 1299. (b) Piton, N.; Schiemann, O.; Mu, Y.; Stock, G.; Prisner, T. F.; Engels, J. W. *Nucleosides Nucleotides Nucl.* **2005**, *24*, 771. (c) Piton, N.; Mu, Y.; Stock, G.; Prisner, T. F.; Schiemann, O.; Engels, J. W. *Nucleic Acids Res.* **2007**, doi:10.1093/nar/gkm169.
(24) (a) Pauly, H. *Justus Liebigs Ann. Chem.* **1902**, *322*, 77. (b) Rozantsev, E. G. In *Free Nitroxyl Radicals*; Ulrich, H., Ed.; Plenum Press: New York, 1970; pp 203.
(25) (a) Kálai, T.; Balog, M.; Jekö, J.; Hideg, K. *Synthesis* **1999**, 973. (b) Schiemann, O.; Piton, N.; Plackmeyer, J.; Bode, B. E.; Prisner, T. F.; Engels, J. W. *Nat. Protoc.* **2007**, *2*, 904.
(26) (a) Schwartz, M. A.; Parce, J. W.; McConnell, H. M. *J. Am. Chem. Soc.* **1979**, *101*, 3592. (b) Brackmann, W.; Gaazbeek, C. J. *Rec. Trav. Chim.* **1966**, *85*, 221.
(27) (a) Ito, H.; Arimoto, K.; Senusui, H.-O.; Rosomi, A. *Tetrahedron Lett.* **1997**, *38*, 3977. (b) Ley, K. D.; Li, Y.; Johnson, J. V.; Powell, D. H.; Schanze, K. *Chem. Commun.* **1999**, 1749.

Scheme 1. Overview of Synthesized Polyradical PELDOR Model Systems

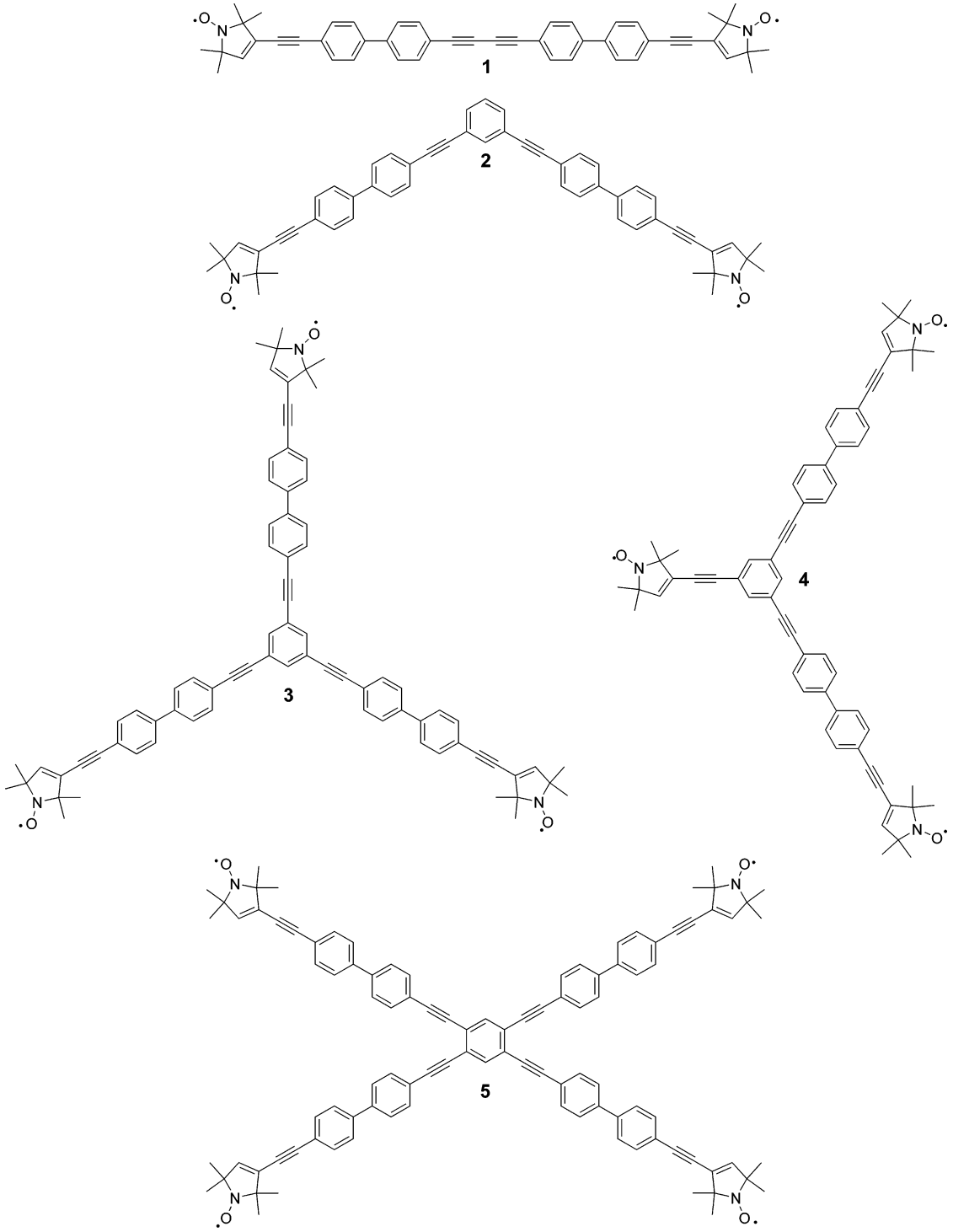

hydroxymethyl because of the lower toxicity of the reagent.[28] Purification of **7** is readily performed, and a 43% yield was obtained.

Nitroxide **6** can be attached to the halogeno-substituted sp^2-carbon atom in **7** by means of transition metal-catalyzed cross coupling reactions such as the Sonogashira coupling.[29] Nitroxides can usually be coupled in high yields (84%)[30] under mild conditions.[31] However, Sonogashira couplings involving 1,3-enynes such as **6** are up to 17% lower in yield than those using nonconjugated terminal acetylenes.[32] Here, the protected precursor **8** was obtained in 74% yield. Molecule **8** was converted to the deprotected[33] precursor **9** in 93% yield by reacting **8** and

(28) (a) Bumagin, N. A.; Ponomaryov, A. B.; Beletskaya, I. P. *Synthesis* **1984**, 728. (b) Kukula, H.; Veit, S.; Godt, A. *Eur. J. Org. Chem.* **1999**, 277.

(29) (a) Khan, S. I.; Grinstaff, M. W. *J. Am. Chem. Soc.* **1999**, *121*, 4704. (b) Takahashi, S.; Kuroyama, Y.; Sonogashira, K.; Hagihara, N. *Synthesis* **1980**, 627. (c) Kálai, T.; Balog, M.; Jekö, J.; Hubbell, W. L.; Hideg, K. *Synthesis* **2002**, 2365. (d) Kirchner, J. J.; Hustedt, E. J.; Robinson, B. H.; Hopkins, P. B. *Tetrahedron Lett.* **1990**, *31*, 593.

(30) Romero, F. M.; Ziessel, R. *Tetrahedron Lett.* **1999**, *40*, 1895.

(31) Sonogashira, K. In *Handbook of organopalladium chemistry for organic synthesis*; Nigishi, E., de Meijere, A., Eds.; Wiley: New York, 2002; Vol. 1, pp 493.

(32) (a) Miller, M. W.; Johnson, C. R. *J. Org. Chem.* **1997**, *62*, 1582. (b) Fritscher, J.; Beyer, M.; Schiemann, O. *Chem. Phys. Lett.* **2002**, *364*, 393.

Scheme 2. Synthesis of Polyradical Precursor **9**[a]

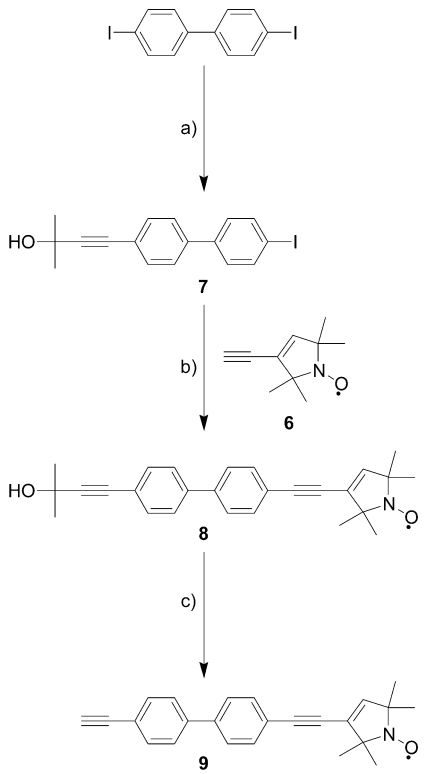

[a] Conditions: (a) $HNEt_2$, benzene, CuI, $PdCl_2(PPh_3)_2$, 2-methyl-3-butyn-2-ol, 43%; (b) NEt_3, piperidine, DMF, CuI, $PdCl_2(C_6H_5CN)_2$, spin-label **6**, 74%; (c) KOH, toluene, 93%.

KOH in toluene at 110 °C.[34] Compound **9** was used without further purification.

The terminal acetylene **9** was then reacted with either 1,3,5-triiodobenzene **10**[35,36] or 1,2,4,5-tetraiodobenzene **11**[37] leading to the symmetric polyradical molecules **3** and **5**, respectively. The asymmetric triradical **4** was obtained by coupling **12**, the reaction product of **6** with **10**, to precursor **9**. Molecules **3**, **4**, and **5** were yielded in 14%, 66%, and 18%, respectively. The low yields upon coupling of more than one acetylene unit to an aromatic system are commonly observed for phenylacetylene systems.[38] Yields of Sonogashira couplings involving nitroxides **6** and **9** could be raised by up to 18% using bis(benzonitrile)-palladium(II)chloride as a catalyst and either triethylamine or a 1:5 mixture of piperidine and triethylamine instead of bis-(triphenylphosphine)palladium(II)chloride in triethyl- or diethylamine (Scheme 3).

The initial attempt to couple **9** two times to **10** to obtain a biradical from the given pool of building blocks failed, as the product could not be isolated as a pure substance. Synthesizing the corresponding non-iodo substituted biradical **2** from 1,3-diiodobenzene also did not succeed again because of problems in purification. We address these purification problems to the dimerization of **9** to the homo-coupling product **1** and further uncharacterized byproducts. The formation of **1** could not be avoided in any Sonogashira coupling using precursor **9**. It can be isolated in a yield of up to 15% following the synthesis of **3**−**5** given in Scheme 3. To overcome these problems, we chose to synthesize 1,3-diethynylbenzene **13**[39] and attach this to the iodo-substitued radical **14** (Scheme 4). In that manner the formation of **1** is excluded and **14** was obtained in 45% yield. The homocoupling products of **13** were readily separated off via column chromatography. (*Note: The colorless oil **13** is known to explode upon attempts of vacuum distillation. **13** should only be distilled at high vacuum and temperatures of less than 60 °C in well-shielded equipment. Only limited quantities should be stored or manipulated as pure, undiluted material*). Molecules **3** and **5** were not prepared using the strategy shown in Scheme 4 because of the increasing reactive character of higher polyethynyl compounds such as 1,2,4,5-tetraethynylbenzene.[40]

Hence, convenient routes to rigid, shape persistent polyradical systems have been established by means of Sonogashira couplings and a corresponding polar protective group strategy. This route is easily extendable to a variety of iodo substituted arylic compounds. In comparison to a synthesis strategy where a spin label bearing an acid functionality is attached via esterification in the final step of the synthesis,[41] less coupling and deprotection steps are needed here. The overall yields are comparable for both strategies.

PELDOR Distance Measurements. The 4-pulse ELDOR time traces of model systems **1**−**5** and the corresponding distances obtained from Tikhonov regularizations[42] are shown in Figure 2. The obtained distances agree well with the predicted ones and are summarized in Table 1. To ensure the reproducibility and significance, the regularization was also performed on longer time traces with higher resolution than shown in Figure 2. No changes in the dominant peaks in the distance domain were observed. Cosine Fourier transformation as an alternative method to extract distances from the time-domain data did not resolve all individual dipolar frequencies in traces d and e as strong peaks (see Supporting Information). Especially in trace e, the full set of three predicted distances could only be recovered by Tikhonov regularization. Provided a high signal-to-noise ratio is obtained and modulations are observed, this procedure is a valuable tool to extract distances. In **4** and **5** all different distances within the molecules could be disentangled even though two distances in **5** differ by 5 Å only.

The linear biradical **1** (trace a) exhibits the largest number of visible oscillations leading to a narrow peak in the distance transformation. In contrast, the bent, meta-substituted molecules

(33) (a) Harris, S. J.; Walton, D. R. M. *Tetrahedron* **1978**, *34*, 1037. (b) Havens, S. J.; Mergenrother, P. M. *J. Org. Chem.* **1985**, *50*, 1763. (c) Swindell, C. S.; Fan, W.; Klimko, P. G. *Tetrahedron Lett.* **1994**, *35*, 4959. (d) Rodriquez, J. G.; Martin-Villamil, R.; Cano, F. H.; Fonesca, I. *J. Chem. Soc., Perkin Trans. I* **1997**, 709.
(34) Ley, K. D.; Li, Y.; Johnson, J. V.; Powell, D. H.; Schanze, K. *Chem. Commun*. **1999**, 1749.
(35) Crystal structure of 1,3,5-triiodobenzene: Margraf, D.; Bats, J. W. *Acta Cryst.* **2006**, *E62*, 502.
(36) Preparation of 1,3,5-triiodobenzene: Schöberl, U.; Magnera, T. F.; Harrison, R. M.; Fleischer, F.; Pflug, J. L.; Schwab, P. F. H.; Meng, X.; Lipiak, D.; Noll, B. C.; Allured, V. S.; Rudalevige, T.; Lee, S.; Michl, J. *J. Am. Chem. Soc.* **1997**, *119*, 3907.
(37) Preparation of 1,2,4,5- tetraiodobenzene: Mattern, D. L. *J. Org. Chem*. **1984**, *49*, 3051.
(38) Jones, C. S.; O'Connor, M. J.; Haley, M. M. In *Acetylene Chemistry*; Diederich, F., Stang, P. J., Tykwinski, R. R., Eds.; Wiley: Weinberg, Germany, 2005; pp 303.
(39) Neenan, T. X.; Whitesides, G. M. *J. Org. Chem*. **1988**, *53*, 2489.
(40) Berris, B. C.; Hovakeemian, G. H.; Lai, Y.-H.; Mestdagh, H.; Vollhardt, K. P. C. *J. Am. Chem. Soc.* **1985**, *107*, 5670.
(41) Godt, A.; Franzen, C.; Veit, S.; Enkelmann, V.; Pannier, M.; Jeschke, G. *J. Org. Chem.* **2000**, *65*, 7575.
(42) (a) Jeschke, G.; Koch, A.; Jonas, U.; Godt, A. *J. Magn. Reson.* **2002**, *155*, 72. (b) Bowman, M. K.; Maryasov, A. G.; Kim, N.; DeRose, V. J. *Appl. Magn. Reson.* **2004**, *26*, 23. (c) Chiang, Y.-W.; Borbat, P. P.; Freed, J. H. *J. Magn. Reson.* **2005**, *172*, 279. The program used for data inversion was obtained from the following: Distance Measurements on Nanoscopic Lengthscales by Pulse EPR. http://www.mpip-mainz.mpg.de/~jeschke/distance.html.

Scheme 3. Synthesis of Polyradical Systems[a]

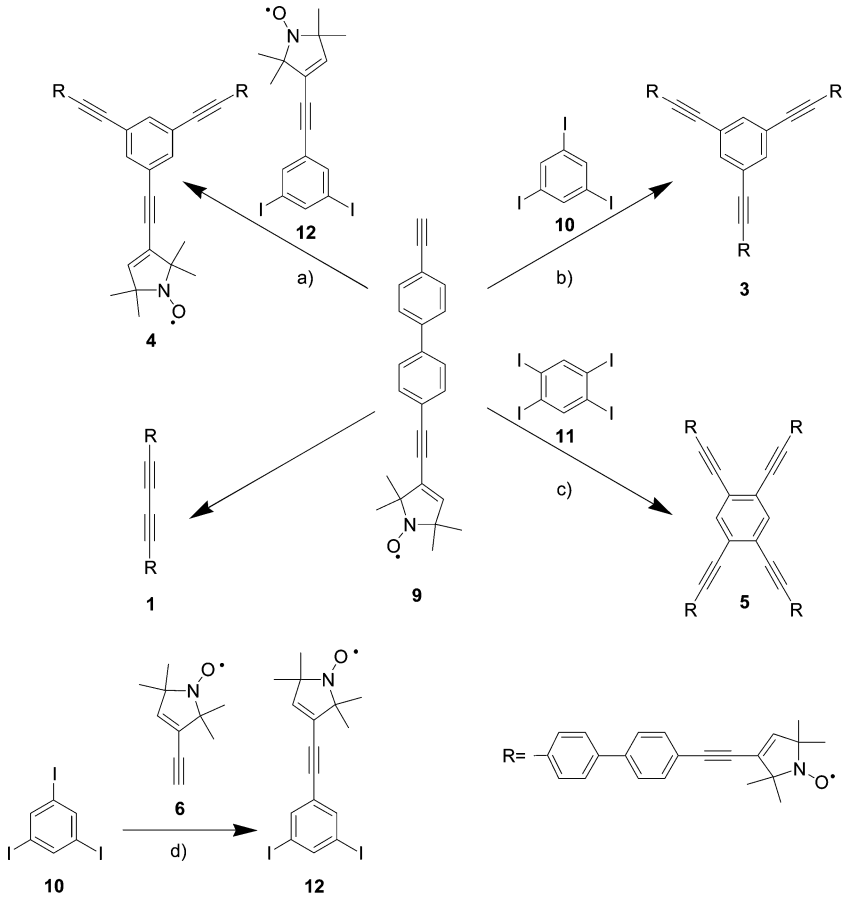

[a] Conditions: (a) NEt_3, DMF, CuI, $PdCl_2(C_6H_5CN)_2$, **12**, 66%; (b) $HNEt_2$, C_6H_6, CuI, $PdCl_2(PPh_3)_2$, **10**, 14%; (c) NEt_3, piperidine, DMF, CuI, $PdCl_2(C_6H_5CN)_2$, **11**, 18%; (d) NEt_3, piperidine, DMF, CuI, $PdCl_2(C_6H_5CN)_2$, spin-label **6**, 32%.

Scheme 4. Synthesis of Biradical **4**[a]

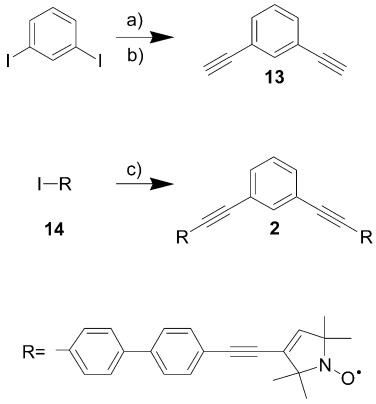

[a] Conditions: a) NEt_3, piperidine, DMF, CuI, $PdCl_2(C_6H_5CN)_2$, trimethylsilylethyne; (b) TBAF, THF; (c) NEt_3, piperidine, DMF, CuI, $PdCl_2(C_6H_5CN)_2$, **13**, 11%.

2 and **3** display faster damping of the oscillations and consequently broader peaks in the distance domain. The different widths of the peaks in the distance domain can be qualitatively related to the molecular structure. In a linear, stretched structure as in **1**, the spin−spin distance can only be reduced by molecular bending motions. Whereas, in bent structures as in **2** and **3** bending motions can increase and decrease the end-to-end distance around the equilibrium structure. Furthermore, the same angular deviations lead to larger distance deviations in a bent structure than in a linear structure based on simple geometric considerations. Consequently, the asymmetric triradical **4** shows peaks of approximately the same widths as for radicals **2** and **3**. The faster damping of the modulation of **4** is due to the interfering dipolar frequencies. The approximately 2-fold higher intensity of the peak at 2.5 nm in the distance domain of asymmetric triradical **4** may also be rationalized by the molecular geometry, the shorter distance can be extracted two times, the longer distance only once. However, tetraradical **5** does not show this correlation. According to structural symmetry all three distances appear two times, but the intensities of the peaks differ. On the other hand the decreasing widths of the peaks at 2.2 (ortho), 3.4 (meta), and 3.8 (para) nm are in agreement with the above considerations about molecular structure and bending motions. Consequently, Tikhonov regularization nicely yields the mean distances, but a quantitative analysis of the distance distribution should be treated with care. The reason is that in current state-of-the-art software implementations the time domain data is only simulated as a sum of pairs and not as a sum of products of triples or quadruples. Therefore, cross-terms of higher order in λ_B arising from the simultaneous pumping of several B spins in tri- and tetraradicals are not properly treated.[42b] Especially, in tetraradical **5** the probability of multiple, coherent B-spin flips is fairly high (∼35%), which might cause the observed regularization artifact and improper amplitudes in the distance distribution.

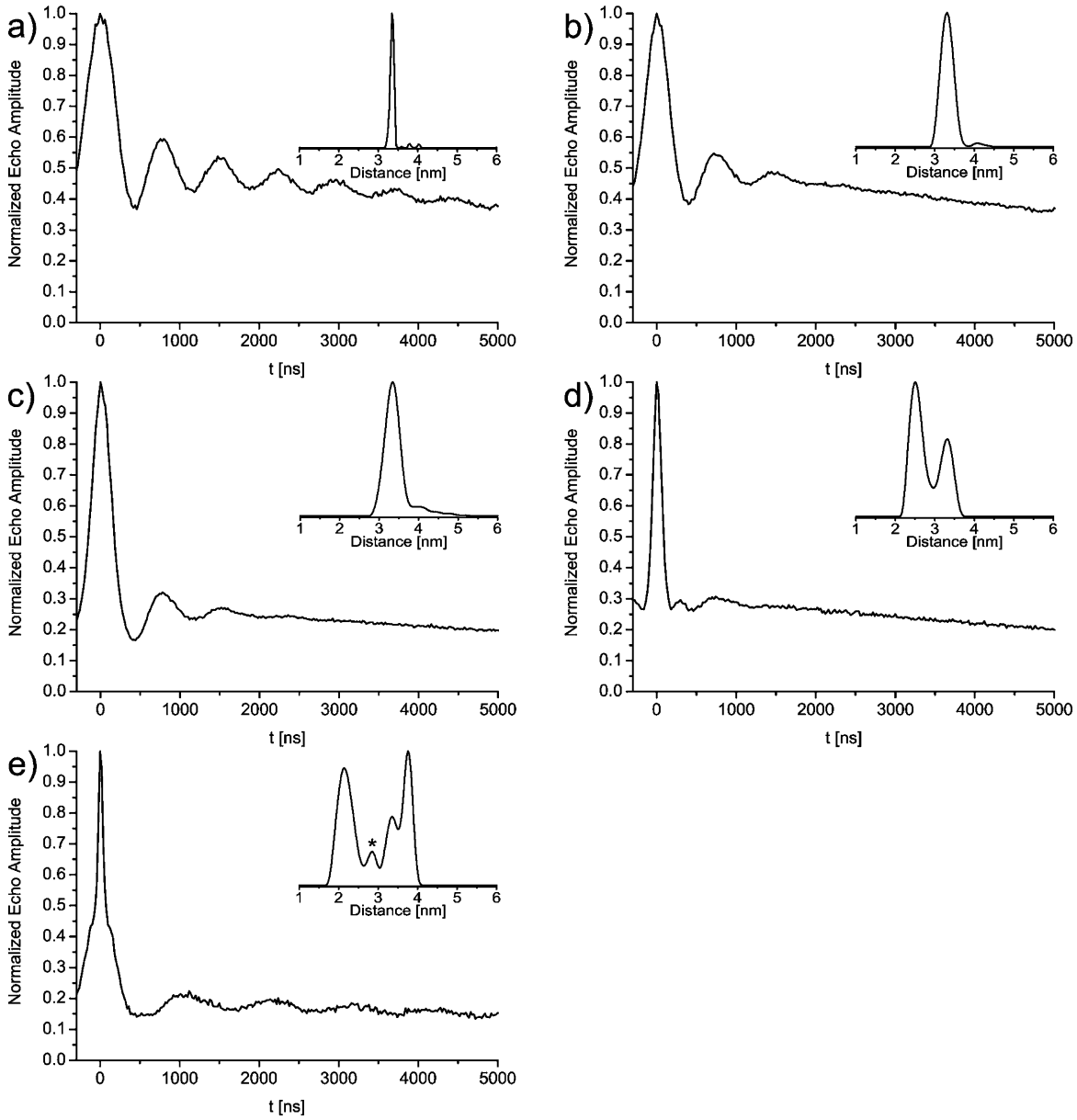

Figure 2. PELDOR trace of model systems **1**, **2**, **3**, **4**, **5** in panels a, b, c, d, e, respectively. Distance transformations from Tikhonov regularizations are shown as inset. The peak marked with an asterisk (∗) in the distance domain of panel e is an artifact from the regularization, which is not significant within the signal-to-noise ratio (see Supporting Information).

Table 1. Distances *r* [nm] from Modeling and Tikhonov Regularization

molecule[a]	modelled *r* [nm][b]	PELDOR *r* [nm][c]
1	3.4	3.4(0.1)
2	3.4	3.3(0.4)
3	3.4	3.3(0.4)
4 [1,3/1,5]	2.5	2.5(0.4)
4 [3,5]	3.4	3.3(0.4)
5 [ortho]	2.0	2.2(0.5)
5 [meta]	3.4	3.3(0.4)
5 [para]	3.9	3.8(0.3)

[a] The numbers in square brackets give the positions at the benzene ring to which the nitroxide bearing moieties are linked to. [b] The values are the distances between the centers of the N−O bonds. [c] The number in brackets is the full width at half-maximum of the corresponding peak.

PELDOR Spin-Counting. We then used molecules **1**−**6** to prove that the number *n* of coupled nitroxides can be determined from the PELDOR time traces, using the analytical expressions derived for geometrically uncorrelated radical centers. On the basis of the considerations of Milov, Tsvetkov et al.[18] (see also Methods and Materials section) the spectra in Figure 2 were corrected for the intermolecular contributions to the echo decay by division by a monoexponential decay and normalized to $t = 0$. The processed spectra are shown in Figure 3.

Figure 3 clearly demonstrates that the modulation depth increases from a mono- to a tetraradical. Reading off the modulation depth V_λ at the end of the respective time traces and substituting the value into eq 7 allows direct determination of the number of spins *n*. The spin-counting results are compared to the actual number of spins in the corresponding molecules in Table 2. Obviously, the experimental spin-counting nicely reproduces the nominal number of spin centers in the model systems. The accuracy in *n* is determined by the error in the modulation depths V_λ. The observed experimental reproducibility of the individual V_λ values is within 0.02 leading to an error in

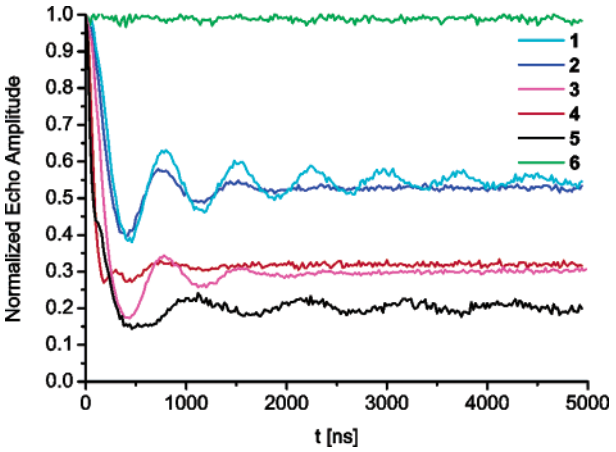

Figure 3. Corrected time domain signals for determination of n in **1**−**6**. V_λ is read off as the echo amplitude at $t = 5000$ ns.

Table 2. Number of Spins n from Processed Time Domain Data

molecule	n	V_λ	n_{found}[a]
1	2	0.54	2.1(1)
2	2	0.53	2.1(1)
3	3	0.30	3.1(2)
4	3	0.32	3.0(2)
5	4	0.20	3.9(2)

[a] The number in brackets is the error in the last digit, determined from a ΔV_λ of 0.02.

n of about 5%. Important for this accuracy is a high signal-to-noise ratio (here >100:1) and a precise value for λ_B. In this study λ_B was calibrated with standard biradicals.[43] Phase cycling of the $\pi/2$-pulse is mandatory to eliminate receiver offsets, because the applied deconvolution of intra- and intermolecular contributions to the echo decay implies that the experimental trace is zero at infinity. In addition, the measured number of spins was independent of the sample concentration and τ-modulation averaging (see Supporting Information). Under these conditions monomers, dimers, trimers, and tetramers can be readily distinguished. Within these limits a pentamer can still be identified, but for $n > 5$ we expect a strong decrease in accuracy, since V_λ will come closer to zero, which lowers the signal-to-noise ratio, and the differences in V_λ decrease with the potency of n.

As mentioned in the Methods and Materials section, V_λ is described as a product of the contributions of all coupled spins (eq 6). Figure 4 shows the applicability of eq 6. The cube root of tetraradical **5** and the square roots of triradicals **3** and **4** give within the error the same V_λ as biradicals **1** and **2**.

In this work we approximated λ_B to be identical in radicals **1**−**6**, which will be valid if the orientations of the nitroxide labels within one molecule, and thus their respective hyperfine and g-tensor orientations, are not correlated with each other. If this assumption was not fulfilled, λ_B would depend on the relative orientation. To verify our assumption of negligible angular correlation, we performed numerical simulations of the time domain signals of linear biradical **1** and bent triradical **3** exhibiting different geometries. Assuming some degree of backbone bending (±10°) and full rotational freedom about the acetylene linkers a set of 10 000 structures was generated. The

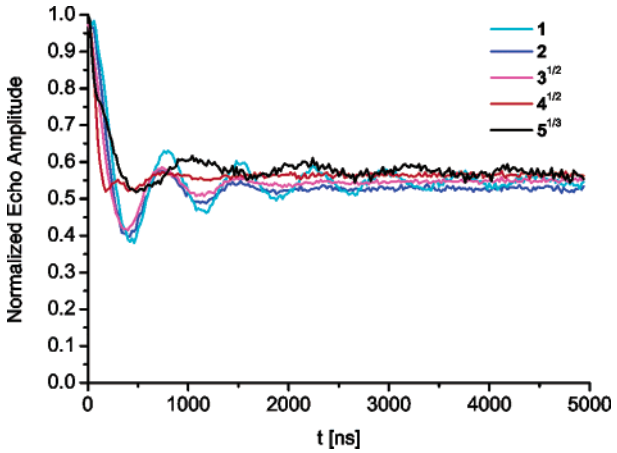

Figure 4. Modulation depths can be described as factorized by the number of coupling spins.

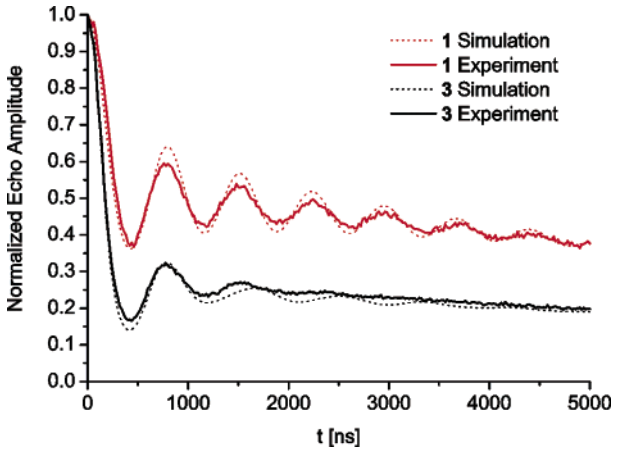

Figure 5. Experimental PELDOR data and simulations for **1** and **3**.

simulations were obtained by explicit calculation of λ_B for each structure and random orientation with respect to the external magnetic field. The result depicted in Figure 5 shows that especially the modulation depth parameters λ_B of the experimental data are reproduced very well. Thus, estimating equal λ_B values is feasible. However, we do not exclude that weak angular correlations might be present, but they are not observed within the error of the experiment. Recent work by Jeschke and co-workers[44] on similar biradical model systems exhibited high flexibility and also weak correlations in label orientations. In biological systems spin labels are usually even more flexible than in this study, so their angular correlation will be even weaker. Thus, it is possible to count the number of monomers in samples of pure oligomeric states, using eq 7.

To verify the linear approximation, leading to eq 8, we increased the inversion pulse length to 92 ns, decreasing λ_B to about 0.12. This pulse is still not long enough to yield a λ_B fulfilling the linear approximation. In addition, data obtained with the 92 ns pump pulse do not meet the accuracy of the 12 ns pulse, even within the factorization approach (eq 7) (see Supporting Information). This longer, more selective inversion pulse introduces several problems: First, its small excitation bandwidth leads to an orientation selectivity of the pumped species causing the absolute error in λ_B to increase as compared

(43) Weber, A.; Schiemann, O.; Bode, B.; Prisner, T. F. *J. Magn. Reson.* **2002**, *157*, 277.

(44) Godt, A.; Schulte, M.; Zimmermann, H.; Jeschke, G. *Angew. Chem., Int. Ed.* **2006**, *45*, 7560.

Table 3. Mixtures and the Corresponding Measured and Calculated V_λ

mixture[a]	V_λ measured[b]	V_λ calculated[c]	V_λ calculated[d]
1+**6** (1)	0.77(2)	0.77	0.79
3+**6** (2)	0.69(2)	0.65	0.68
4+**6** (2)	0.75(2)	0.65	0.74
5+**6** (3)	0.76(2)	0.61	0.74
1+**3** (1)	0.43(2)	0.42	0.42
1+**5** (2)	0.43(2)	0.37	0.41

[a] The number in brackets gives the difference in n between the two molecules. [b] The number in brackets gives the error in the last digit. [c] These numbers are calculated with eq 9. [d] These numbers are calculated with eq 10.

to the short pulse by amplification of the effects of small angular correlations. Second, the differences in V_λ become smaller with decreasing λ_B, which raises the overall uncertainty in n. Finally, in the case of different dipolar coupling strengths, as present in our model systems, λ_B will show a dependence on the coupling.[45] This dependence can be neglected only if the microwave field strength B_1 is much larger than the dipolar coupling, which is here fulfilled better for the 12 ns pulse as compared to the 92 ns pulse. However, a long inversion pulse might be useful for aggregates with a large number of spin-bearing centers.[46]

Since biological systems may exhibit an equilibrium between monomers, dimers, and higher oligomers, we prepared various mixtures of mono-, bi-, tri-, and tetraradicals equimolar in spin concentrations and measured the resulting PELDOR spectra (Table 3, Figure S4 in Supporting Information).

The analysis of these data is complicated, because n in eq 7 cannot simply be substituted by the average number of spins $\bar{n}$ (see also Supporting Information Table S4). The substitution with $\bar{n}$ would only be valid, if the linear approximation leading to eq 8 was fulfilled. Instead the resulting signal is the sum of responses of different species and eq 6 transforms to eq 9, where x_i is the fraction of spins in the respective oligomer giving the signal $V_{\lambda i}$.

$$V_\lambda = \sum_i x_i V_{\lambda i} \tag{9}$$

In column 3 of Table 3 the V_λ of each mixture is calculated using eq 9, which are the weighted sums of the signals of the pure substances. Comparison with the experimental results shows that the data are not reproduced for mixtures with large differences in the number of coupled spins per molecule. We attribute this to different transversal relaxation induced by the dipolar couplings within the oligomers. Therefore, the proper weighting factors also have to contain the contribution of each oligomer to the refocused echo intensity. This difference in transversal relaxation is taken explicitly into account by the scaling factor s_i yielding eq 10 (for details see Supporting Information).

$$V_\lambda = \frac{\sum_i s_i x_i V_{\lambda i}}{\sum_i s_i x_i} \tag{10}$$

Column 4 in Table 3 shows the results for the six mixtures according to eq 10. The calculated values are now in agreement with the experimental data, indicating the importance of relaxation for mixtures.

In samples of unknown composition this analysis becomes more demanding, because the fraction of each oligomer and its respective dipolar relaxation enhancement are unknown. In this case, studying V_λ as a function of λ_B[18a,46] might allow an extraction of the constituents of the mixture, assuming a high enough signal-to-noise ratio. Furthermore, extraction of V_λ as a function of the observation time window τ_2 might allow extrapolation of the dipolar relaxation scaling factors of the different oligomers. Therefore, with a series of measurements, the dependencies of V_λ on λ_B and τ_2 might be determined and the composition of unknown mixtures derived.

Prior to this experimental validation of spin-counting, the method had already been applied to biological systems of known oligomerization states,[47] but the data did in neither case reproduce the oligomeric states found in crystal structures or by biochemical methods. These discrepancies might be attributed to experimental noise, incomplete spin labeling, and/or mixtures of oligomeric states.

Comparison with Other Methods. Another EPR based method for nanometer distance measurements is the excitation of double quantum coherences (DQC).[48] However, this method is technically more demanding, because the full EPR-spectra have to be excited and the nature of the experiment does not allow counting the number of spins in a cluster easily.

In comparison to high-resolution NMR, dynamic light scattering, fluorescence spectroscopy, or ESI that can all be performed in solution under native conditions, PELDOR measurements need to be performed in immobilized samples, usually glassy frozen solutions. On the other hand, PELDOR is not restricted in system size; measurements can be performed in membranes and yield in the same experiment not only the number of constituting monomers but also precise information about their geometric arrangement. The method is comparable to spin−spin distance measurements in solid-state NMR, for example, REDOR; however, owing to the higher magnetic moment of electron spins, distances of up to 80 Å are accessible by PELDOR.

Conclusion

We have shown on a variety of newly synthesized polyradicals that a single PELDOR data set yields not only distances, and thereby precise geometric information on the nanometer scale, but also the number of spins n in a molecule. The method has an overall error of ~5% in n for up to four spins, provided that the spin-labeling is complete and that the error of the excitation probability factor λ_B does not exceed 0.02, which can be readily achieved. In complexes with more than five spins, with incomplete labeling, or in the presence of mixtures of oligomeric states this accuracy strongly decreases. Mixtures of

(45) Jeschke, G.; Chechik, V.; Ionita, P.; Godt, A.; Zimmermann, H.; Banham, J.; Timmel, C. R.; Hilger, D.; Jung, H. *Appl. Mag. Reson.* **2006**, *30*, 473.
(46) Bowman, M. K.; Becker, D.; Sevilla, M. D.; Zimbrick, J. D. *Radiat. Res.* **2005**, *163*, 447.
(47) (a) Jeschke, G.; Bender, A.; Schweikardt, T.; Panek, G.; Decker, H.; Paulsen, H. *J. Biol. Chem.* **2005**, *280*, 18623. (b) Hilger, D.; Jung, H.; Padan, E.; Wegener, C.; Vogel, K.-P.; Steinhoff, H.-J.; Jeschke, G. *Biophys. J.* **2005**, *89*, 1328. (c) Banham, J. E.; Timmel, C. R.; Abbott, R. J. M.; Lea, S. M.; Jeschke, G. *Angew. Chem., Int. Ed.* **2006**, *45*, 1058.
(48) (a) Borbat, P. P.; Mchaourab, H. S.; Freed, J. H. *J. Am. Chem. Soc.* **2002**, *124*, 5304. (b) Borbat, P. P.; Davis, J. H.; Butcher, S. E.; Freed, J. H. *J. Am. Chem. Soc.* **2004**, *126*, 7746. (c) Dzikovski, B. G.; Borbat, P. P.; Freed, J. H. *Biophys. J.* **2004**, *87*, 3504. (d) Pornsuwan, S.; Bird, G.; Schafmeister, C. E.; Saxena, S. *J. Am. Chem. Soc.* **2006**, *128*, 3876.

oligomeric states could be analyzed by measuring V_λ as a function of λ_B, with the limitations described herein. Thus, PELDOR is a method by which the oligomeric state of biologically relevant complexes can be evaluated down to concentrations of $\sim$50 μM at a volume of 80 μL, given that the monomers carry a spin center, and that the spin−spin distances are within the PELDOR limit (15−80 Å).

Acknowledgment. We acknowledge Prof. Dr. Christoph Elschenbroich, Philipps-University Marburg, for recording EI mass spectra, Dr. Ute Bahr, Johann Wolfgang Goethe-University, for recording ESI and MALDI mass spectra and Prof. Dr. Snorri Th. Sigurdsson for discussion. We thank reviewer 2 and reviewer 4 for helpful discussions about applicability and limitations of the analytical expressions used. This work has been supported by the Center for Biomolecular Magnetic Resonance Frankfurt and the Deutsche Forschungsgemeinschaft (SFB 579 ("RNA - ligand interactions") and SCHI 531-5/2). D.M. is grateful for a CMP fellowship.

Supporting Information Available: Detailed experimental procedures, all Fourier transformed PELDOR spectra, spectra with proton modulation suppression, spectra of mixtures, PELDOR data with a low λ_B pump pulse, and concentration dependence. This material is available free of charge via the Internet at http://pubs.acs.org.

JA065787T